

# ChemComm

Accepted Manuscript



This is an *Accepted Manuscript*, which has been through the Royal Society of Chemistry peer review process and has been accepted for publication.

*Accepted Manuscripts* are published online shortly after acceptance, before technical editing, formatting and proof reading. Using this free service, authors can make their results available to the community, in citable form, before we publish the edited article. We will replace this *Accepted Manuscript* with the edited and formatted *Advance Article* as soon as it is available.

You can find more information about *Accepted Manuscripts* in the [Information for Authors](#).

Please note that technical editing may introduce minor changes to the text and/or graphics, which may alter content. The journal's standard [Terms & Conditions](#) and the [Ethical guidelines](#) still apply. In no event shall the Royal Society of Chemistry be held responsible for any errors or omissions in this *Accepted Manuscript* or any consequences arising from the use of any information it contains.

## Fusion and Planarization of BisBODIPY: a New Family of Photostable Near Infrared Dyes

Received 00th January 20xx,  
Accepted 00th January 20xx

Changjiang Yu,<sup>a</sup> Lijuan Jiao,<sup>\*a</sup> Tingting Li,<sup>a</sup> Qinghua Wu,<sup>a</sup> Wei Miao,<sup>a</sup> Jun Wang,<sup>a</sup> Yun Wei,<sup>a</sup> Xiaolong Mu<sup>a</sup> and Erhong Hao<sup>\*a</sup>

DOI: 10.1039/x0xx00000x

www.rsc.org/

We have synthesized a new family of directly-fused bisBODIPY BBP **1** through a key FeCl<sub>3</sub>-mediated intramolecular oxidative cyclodehydrogenation reaction and its derivatives **2** and **3** from the Knoevenagel reaction. These dyes display effective expansion of  $\pi$ -conjugation over the two BODIPYs due to their locked coplanar conformation, showing intriguing electrochemical and spectroscopic properties, such as intensive absorption/emission bands ranging from 676 to 877 nm and high photostability.

Near-infrared (650–900 nm, NIR) dyes have found widespread applications in non-invasive and in vivo fluorescence imaging, ranging from various biological systems to material science<sup>1</sup>. The classical boron dipyrromethene (BODIPY) skeleton absorbs and emits around 500 nm,<sup>2,3</sup> but exhibits promising because of their advantageous spectroscopic and chemical properties, such as relatively high fluorescence quantum yields, large molar extinction coefficients and sharp fluorescence peaks, coupled with chemical versatility and color tunability. Various structural modifications on BODIPY have been summarized to obtain far-red and NIR derivatives<sup>2</sup>, mainly by introducing linear aromatic groups<sup>4</sup>, cyclic aromatic groups<sup>5</sup>, N replacing *meso*-C<sup>6</sup> and conjugated oligomers<sup>7–9</sup>.

Recently, several BODIPY conjugated oligomers with fused structures have been synthesized showing intensive NIR absorption/emission bands due to the expansion of  $\pi$ -conjugation. Wakamiya and Yamaguchi<sup>7</sup> developed  $\alpha$ ,  $\alpha$ -benzene fully fused bisBODIPY **A** (Figure 1) as stable NIR dyes. Nagata and Uno<sup>8</sup> developed  $\beta$ ,  $\beta$ -benzene  $\pi$ -fused bisBODIPY **B** (Figure 1) as promising candidates for NIR-selective dyes. Hiroto and Shinokubo<sup>9</sup> reported pyrazine fused BODIPY trimer with NIR absorption through the oxidation of corresponding  $\beta$ -amino BODIPY. However, these dyes all need comprehensive

synthesis. On the other hand, the readily available bisBODIPY **C**<sup>10a–b</sup> directly linked at  $\beta$ ,  $\beta$ -positions (Figure 1) exhibits twisted conformation with a dihedral angle of 64.1(1)°, and thus the  $\pi$  conjugation is blocked between one BODIPY structure and another due to the steric hindrance of methyl substituents. The  $\beta$ -directly linked bisBODIPY<sup>10c</sup> without steric interaction exhibits effective  $\pi$ -conjugation and a coplanar conformation but its conformation is flexible.

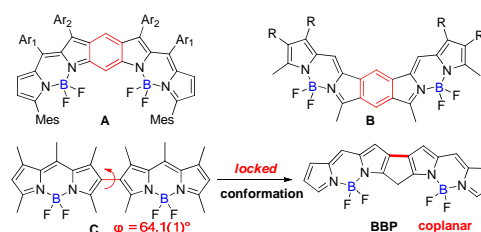
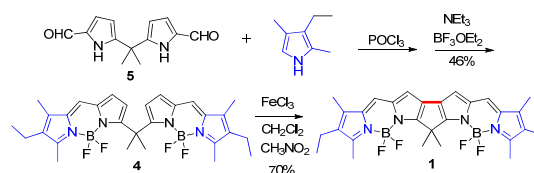


Figure 1. Representative examples of fused bisBODIPYs.

Herein, we report a novel family of highly conjugated directly-fused bisBODIPY (BBP) **1** (Figure 1) with locked coplanar conformation through a key FeCl<sub>3</sub>-mediated intramolecular oxidative cyclodehydrogenation reaction<sup>11–12</sup>. BBP **1** and their postfunctional derivatives **2a/b** and **3a/b** from the Knoevenagel condensation reaction have intensive absorption bands and strong emission in the NIR region (ranging from 676 to 877 nm) and good photostability.



Scheme 1. Syntheses of BBP **1**.

Initially, the carbon-bridged bisBODIPY **4** was synthesized in 46% yield by condensation readily available precursor **5**, 5-(2,4-dimethyl-1,9-diformyldipyrromethane) **5**<sup>13</sup> with 3-ethyl-2,4-dimethylpyrrole and subsequent BF<sub>2</sub> complexation (Scheme 1).

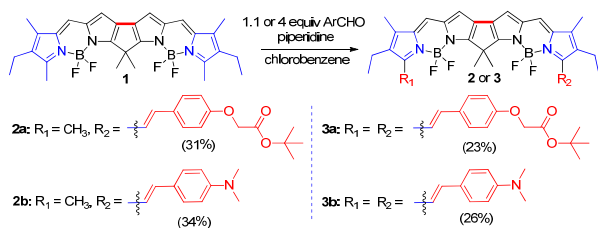
<sup>a</sup> The Key Laboratory of Functional Molecular Solids, Ministry of Education; Anhui Laboratory of Molecule-Based Materials; School of Chemistry and Materials Science, Anhui Normal University, Wuhu, Anhui, China 241000.

\*ljiao421@mail.ahnu.edu.cn, haoehong@mail.ahnu.edu.cn

Electronic Supplementary Information (ESI) available: Experimental details, synthetic procedures and characterization data of all new compounds, additional spectroscopic data, X-ray crystallographic data, and DFT calculation details. See DOI: 10.1039/x0xx00000x

The key bisBODIPY **4** was then subjected to the FeCl<sub>3</sub>-promoted intramolecular oxidative cyclodehydrogenation reaction. The reaction was monitored by TLC. We were delighted to find that the starting bisBODIPY **4** consumed completely and generated a new cyan product at the same time, which was further confirmed to be the directly-fused BBP **1** by X-ray diffraction results, NMR and HRMS. By optimizing the reaction conditions, the directly-fused BBP **1** was generated in 70% yield with 10 equiv of FeCl<sub>3</sub> in anhydrous dichloromethane.

The Knoevenagel condensation reaction<sup>14</sup> of BBP **1** with 1.1 equiv tert-butyl-2-(4-formylphenoxy)acetate or 4-N,N-dimethyl benzaldehyde generated monofunctional bisBODIPYs **2a/b** in 31% and 34% yields (Scheme 2), respectively. When increasing to 4 equiv corresponding aldehyde, we obtained the distyryl-substituted bisBODIPYs **3a/b** in 23 and 26% yields (Scheme 2), respectively.



**Scheme 2.** Syntheses of BBPs **2a-b** and **3a-b** from **1** through the Knoevenagel condensation reaction

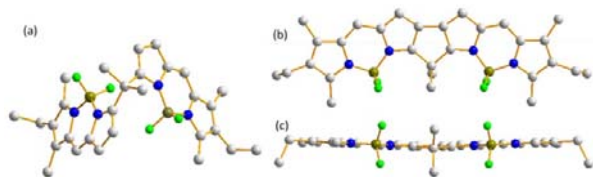


**Figure 2.** (a) X-Ray structures of bisBODIPY **4** and top (a) and front (b) view of BBP **1**. C, light gray; N, blue; B, dark yellow; F, bright green. Hydrogen atoms have been removed for clarity.

The single-crystal molecular structure of the carbon-bridged bisBODIPY **4** reveals a dihedral angle of 76.2(1)° between the mean planes of the two indacene units (Figure 2a), which is more twisted than dihedral angle of 64.1(1)° of bisBODIPY **C** in Figure 1. After locking β, β-positions of the carbon-bridged bisBODIPY **4**, we observed a new five-membered-ring formation in the structure of BBP **1** (Figure 2), resulting in a molecule that has a reflect plane (C<sub>2v</sub> symmetry). X-ray crystallographic analysis reveals a high planarity of seven rigid planar ring structures in the chromophore of BBP **1**: five five-membered-ring units at the periphery and two six-membered-ring units, each incorporating a BF<sub>2</sub> group, with only fluorine atoms and the alkyl substituents deviating from the plane chromophore. The dihedral angle of two pyrrole rings neighbouring newly formed five-membered-ring is 4.7(1)°. BBP **1** exhibits well-ordered crystal stacking slipped in head-to-tail configuration connected by multiple intramolecular and intermolecular C-H...F hydrogen bonds between F atoms and various hydrogen atoms (Figures S2c, ESI), in which the interplanar distance of two molecules is 3.35 Å.

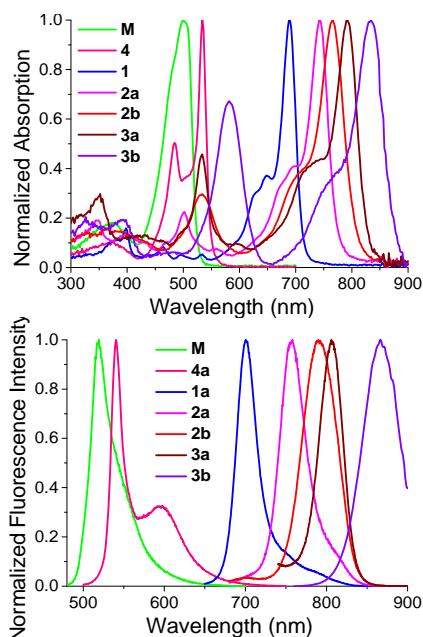


**Figure 3.** Normalized UV-Vis (top) and fluorescence (bottom) spectra of BODIPY **M**, BBPs **1-3**, and bisBODIPY **4** in dichloromethane

The broadened shapes of absorption and emission bands and relatively large Stokes shifts reaching 2000 cm<sup>-1</sup> for **4** (Table S1 and Figure S4, ESI) were observed, with respect to those of monomeric BODIPY **M** (Table S1 and Figure S3, ESI). For example, in contrast to the UV-Vis spectrum of BODIPY **M** (λ<sub>abs</sub><sup>max</sup> 500 nm), the absorption band of **4** is broadened and split into two bands at 484 nm and 534 nm in dichloromethane (Figure S4, ESI). The 484 nm band is slightly blue shifted and the 534 nm band is red-shifted than those of β, β-linked bisBODIPYs<sup>10</sup>. These results are in agreement with the reported bisBODIPYs<sup>15-17</sup>, which has minimal ground-state interaction or excitonic coupling between the two chromophores. Excitation spectra (Figure S10, ESI), recorded on the maximum emission wavelength at 600 nm of bisBODIPY **4**, perfectly match the absorption spectra, indicating a genuine emission of the dimeric species. **4** exhibits high molar absorption coefficients (109000 M<sup>-1</sup>cm<sup>-1</sup>) in dichloromethane and a strong dependence on solvent polarity with fluorescence quantum yield ranging from 0.19 in hexane to 0.17 in dichloromethane and 0.06 in MeOH. The fluorescence lifetime of bisBODIPY **4** gave a lifetime of 1 ns for the 540 nm emission and 2 ns for the 600 nm emission under the same excited wavelength of 485 nm. The two chromophore moieties of **4** which were flexible linked to each other by a carbon-bridge may form an intramolecular excimer due to conformational changes upon excitation. Similar dual emission has been reported for xanthene linked BODIPY dimers<sup>18a</sup> and flexible linked BODIPYs in organized media like micelles.<sup>18b</sup>

After locking coplanar conformation, BBP **1** exhibits relatively high molar absorption coefficients (149600 M<sup>-1</sup>cm<sup>-1</sup>), intensive absorption and emission bands in the NIR region in several solvents studied as summarized in Figure 3, Table S1 and Figures S5 (see ESI). For example, in comparison with those of BODIPY **M**, BBP **1** exhibits the maximum absorption and emission wavelength red-shifted 188 nm and 182 nm,

respectively. Compared with those of bisBODIPY **4**, the maximum absorption and emission wavelength red shifted 154 nm and 105 nm for **1** respectively while they still maintain a relatively small Stokes shift value own to their rigid and almost flat structures. The fluorescence quantum yields of BBP **1** are only slight solvent dependent in either polar or non-polar solvents such as 0.45 in hexane, 0.55 in toluene, 0.54 in dichloromethane, 0.57 in THF and 0.31 in acetonitrile.

Absorption spectra of the Knoevenagel condensation products **2a/b** and **3a/b** exhibit a significant red-shift of the absorption and emission maxima as shown in Figure 3, Table S1 and Figures S6-9 (see ESI). For example, the absorption maxima wavelengths of them in dichloromethane were found to be 744, 766, 792 and 834 nm for BBPs **2a**, **2b**, **3a** and **3b**, respectively. With respect to those of BBP **1**, BBP **3a** shows a 104 and 106 nm red-shift in their absorption and fluorescence emission spectra, respectively. Similar red-shifts are observed for BBPs **2a**, **2b** and **3b**. Unlike BBP **1**, BBP **2** and BBP **3** show solvent-dependent fluorescence as shown in Table S1 and Figures S6-S9 (see ESI). For example, **3a** emits at 804 nm with fluorescence quantum yield of 0.27 in hexane with a reduced fluorescence quantum yield of 0.03 emitting at 796 nm in acetonitrile. This indicates the presence of an intramolecular charge transfer (ICT) process, similar to those previously reported dialkylamino-functionalized BODIPYs<sup>14</sup>. Although the fluorescence quantum yields of **2a** decrease slightly as the polarity of the solvent increases, it remains relatively good in DMSO (0.11), comparative with commercially available dye ICG. In addition, **2b** and **3b** are sensitive to the pH variation of the system.

The addition of TFA to their dichloromethane solutions induced a blue-shift of absorption from 766 nm and 533 nm to 740 and 496 nm for BBP **2b** and from 834 nm and 581 nm to 786 nm and 523 nm for BBP **3b** (Figures S13-14, ESI) due to the protonation of NMe<sub>2</sub> group. To further explore the absorption spectral responses of BBP **2b** and **3b** to acid analyte, an acetonitrile solution of BBP **2b** and **3b** were titrated by the sequential addition of aliquots of trifluoroacetic acid (TFA), which revealed spectacular spectral shifts (Figures S11-12, ESI). Upon absorption addition of TFA for BBP **2b** (Figure S11), a stepwise disappearance of the 750 nm and 527 nm bands and formation of a new band at 725 nm and 490 nm were observed. The sharp isosbestic point at 735 nm and 499 nm indicated the formation of the mono-protonated BBP **2b**-H<sup>+</sup>. A remarkable fluorescence enhancement was also observed during the above titration (Figures S11-12, ESI).

The cyclic voltammetry of newly constructed BBPs **1-3**, bisBODIPY **4** and BODIPY **M** were studied in deoxygenated dichloromethane at room temperature containing tetrabutylammonium hexafluorophosphate (TBAPF<sub>6</sub>) as the supportive electrolyte. As shown in Figure 4 and Table 1, BODIPY **M** exhibits an irreversible reduction wave with  $E_{pc}$  at -1.01 eV and an irreversible oxidation wave with  $E_{pa}$  at 1.31 eV. Compared with the wave of **M**, bisBODIPY **4** increases a reversible reduction wave with half-wave potentials at -1.43 V and an irreversible reduction wave with  $E_{pc}$  at -1.27 eV. Unlike **4**, the BBPs **1a**, **2a** and **3a** display a reversible reduction wave

with half-wave potentials at -1.48, -1.49 and -1.33 eV (vs SCE), a reversible oxidation wave with half-wave potentials at 0.77, 0.69 V and 0.66 V (vs SCE), an irreversible oxidation wave and an irreversible reduction wave with  $E_{pc}$  at -1.53, -1.55 and -1.36 eV (vs SCE), respectively. The split two mono-electronic reduction processes for bisBODIPYs **4**, **1**, **2a** and **3a** indicate the dimeric nature of these compounds by electronic communication between the subunits.<sup>15a,16b</sup> HOMO energy levels of -5.35, -5.11, -5.03, -5.02 eV (vs SCE) and LUMO energy levels of -3.25, -3.46, -3.56, -3.60 eV (vs SCE) were estimated for **4**, **1**, **2a** and **3a**, respectively based on their onset potential of the first oxidation and reduction waves. Thus, the fusion of the two BODIPY and the introduction of corresponding styryl or distyryl help the decrease the LUMO levels and the increase the HOMO levels of the chromophore, resulting in the decrease of the energy band gaps. Electrochemical energy band gaps for **4**, **1**, **2a** and **3a** are 2.10, 1.65, 1.47 and 1.42 eV, respectively.

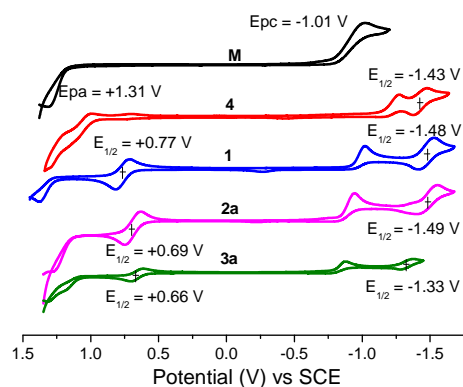


**Figure 4.** Cyclic voltammograms of BODIPY **M**, BBPs **1-3**, and bisBODIPY (**1mM**) measured in dichloromethane and the scan rate at 20 mV s<sup>-1</sup>.

**Table 1.** Electrochemical data acquired and HOMO-LUMO Gaps determined from spectroscopy of BODIPY **M**, BBPs **1-3**, and bisBODIPY **4**.

|           | $E_{red}^1$<br>(V) | $E_{red}^2$<br>(V) | $E_{red}^{onset}$<br>(V) | $E_{ox}^{onset}$<br>(V) | LUMO<br>(eV) | HOMO<br>(eV) | $E_g^3$ (eV) |
|-----------|--------------------|--------------------|--------------------------|-------------------------|--------------|--------------|--------------|
| <b>M</b>  | -1.01              | -                  | -0.82                    | 1.22                    | -3.58        | -5.62        | 2.04         |
| <b>4</b>  | -1.27              | -1.47              | -1.15                    | 0.95                    | -3.25        | -5.35        | 2.10         |
| <b>1</b>  | -1.02              | -1.53              | -0.94                    | 0.71                    | -3.46        | -5.11        | 1.65         |
| <b>2a</b> | -0.94              | -1.55              | -0.84                    | 0.63                    | -3.56        | -5.03        | 1.47         |
| <b>3a</b> | -0.88              | -1.36              | -0.80                    | 0.62                    | -3.60        | -5.02        | 1.42         |

$E_{red}^1$ ,  $E_{red}^2$  = irreversible reduction peak potentials;  $E_{red}^{onset}$  = the onset reductive potentials;  $E_{LUMO} = -e(E_{red}^{onset} + 4.4)$ ;  $E_{ox}^{onset}$  = the onset oxidative potential;  $E_{HOMO} = -e(E_{ox}^{onset} + 4.4)$ ;  $E_g^3 = E_{LUMO} - E_{HOMO}$

DFT calculations indicate both HOMO and LUMO orbitals of BBP **1** are well distributed over the two BODIPY core except the periphery alkyl groups (Figure 5). From **4** to **1**, the calculated HOMO energy levels increase from -4.88 to -4.73 eV, while the LUMO energy levels decrease from -2.51 to -2.85 eV. This trend is in good agreement with the electrochemical data acquired. The calculated decreased energy gap of 0.49 eV from **4** to **1** also explains the 154 nm redshifts of the absorption maximum. Time dependent DFT calculations on BBP **1** show

the sharp and strong absorption with the lowest energy mostly consist of simple HOMO-LUMO transition (the  $S_0$  to  $S_1$  excitation energy is 631 nm and oscillator strength is 1.0936). Additionally,  $S_0$  to  $S_2$  transition with excitation energy of 552 nm might explain the experimental shoulder peaks around 649 nm for BBP **1** (Figure 5a).

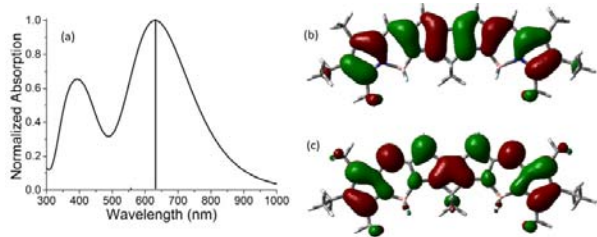


**Figure 5.** (a) DFT calculated absorption spectra of directly fused BBP **1**. The insert lines stand for the oscillator strength; (b) HOMO and (c) LUMO of BBP **1** calculated at the TPSSH/6-31G(d) level

To test their potential practical applications as novel dyes, we also measured the photostabilities of these resultant complexes in DMSO under continuous irradiation with a 500 W Xe lamp. As demonstrated by BBPs **2a** and **3a** in Figure S15 (see ESI), our new dyes show excellent photostability during the period of strong irradiation (40 min): more than 98% amount of BBPs **2a** and **3a** remained, while only 58% of ICG left under the same condition. The high photostabilities of BBP dyes match with previous benzo[*b*]-fused bisBODIPY<sup>7</sup>.

In conclusion, we have developed a new family of BBP dyes **1** and its derivatives **2** and **3**. A key FeCl<sub>3</sub>-mediated intramolecular oxidative cyclodehydrogenation was developed to fuse bisBODIPY **4** to BBP **1** with locked coplanar conformation. These BBP dyes show intriguing electrochemical and useful spectroscopic properties such as intensive absorption bands and emission ranging from 676 nm to 877 nm and high photostability. Further synthesis and applications of these fused bisBODIPY dyes will be reported in due course.

This work is supported by the National Nature Science Foundation of China (Grants Nos. 21372011, 21402001 and 21472002), Nature Science Foundation of Anhui Province (Grants No 1508085J07).

## Notes and references

- (a) L. Yuan, W. Lin, K. Zheng, L. He and W. Huang, *Chem. Soc. Rev.*, 2013, **42**, 622; (b) V. V. Roznyatovskiy, C. H. Lee and J. L. Sessler, *Chem. Soc. Rev.*, 2013, **42**, 1921; (c) Y. Ding, Y. Tang, W. Zhu and Y. Xie, *Chem. Soc. Rev.*, 2015, **44**, 1101.
- (a) A. Loudet and K. Burgess, *Chem. Rev.*, 2007, **107**, 4891; (b) G. Ulrich, R. Ziessel and A. Harriman, *Angew. Chem. Int. Ed.*, 2008, **47**, 1184; (c) N. Boens, V. Leen and W. Dehaen, *Chem. Soc. Rev.*, 2012, **41**, 1130; (d) T. Kowada, H. Maeda and K. Kikuchi, *Chem. Soc. Rev.*, 2015, **44**, 4953; (e) A. C. Benniston and G. Copley, *Phys. Chem. Chem. Phys.*, 2009, **11**, 4124; (f) H. Lu, J. Mack, Y. Yang and Z. Shen, *Chem. Soc. Rev.*, 2014, **43**, 4778; (g) Y. Ni and J. Wu, *Org. Biomol. Chem.*, 2014, **12**, 3774.
- (a) D. Su, J. Oh, S. Lee, J. M. Lin, S. Sahu, X. Yu, D. Kim and Y. Chang, *Chem. Sci.*, 2014, **5**, 4812; (b) S. Choi, J. Bouffard and Y. Kim, *Chem. Sci.*, 2014, **5**, 751; (c) F. Wang, L. Zhou, C. Zhao, R. Wang, Q. Fei, S. Luo, Z. Guo, H. Tian and W. Zhu, *Chem. Sci.*, 2015, **6**, 2584.
- (a) V. Leen, E. Braeken, K. Luckermans, C. Jackers, M. Van der Auweraer, N. Boens and W. Dehaen, *Chem. Commun.*, 2009, **30**, 4515; (b) L. Jiao, C. Yu, T. Uppal, M. Liu, Y. Li, Y. Zhou, E. Hao, X. Hu and M. G. H. Vicente, *Org. Biomol. Chem.*, 2010, **8**, 2517; (c) N. Zhao, S. Xuan, F. R. Fronczek, K. M. Smith, M. G. H. Vicente, *J. Org. Chem.*, 2015, **80**, 8377; (d) N. Zhao, M. Cui, M. G. H. Vicente, F. R. Fronczek, K. M. Smith, *Chem. Eur. J.*, 2015, **21**, 6181.
- (a) K. Umezawa, Y. Nakamura, H. Makino, D. Citterio and K. Suzuki, *J. Am. Chem. Soc.*, 2008, **130**, 1550; (b) K. Umezawa, A. Matsui, Y. Nakamura, D. Citterio and K. Suzuki, *Chem. Eur. J.*, 2009, **15**, 1096; (c) S. G. Awuah, J. Polreis, V. Biradar and Y. You, *Org. Lett.*, 2011, **13**, 3884; (d) C. Yu, Y. Xu, L. Jiao, J. Zhou, Z. Wang and E. Hao, *Chem. Eur. J.*, 2012, **18**, 6437; (e) Y. Ni, W. Zeng, K. Huang and J. Wu, *Chem. Commun.*, 2013, **49**, 1217; (f) W. Zhang, B. Wang, C. Li, J. Zhang, C. Wan, J. Huang, J. Liu, Z. Shen and Y. You, *Angew. Chem. Int. Ed.*, 2015, **54**, 9070.
- (a) W. Zhao and E. M. Carreira, *Angew. Chem., Int. Ed.*, 2005, **44**, 1677; (b) A. Loudet, R. Bandichhor, K. Burgess, A. Palma, S. O. McDonnell, M. J. Hall and D. F. O'Shea, *Org. Lett.*, 2008, **10**, 4771; (c) H. Lu, S. Shimizu, J. Mack, Z. Shen and N. Kobayashi, *Chem. Asian J.*, 2011, **6**, 1026; (d) J. Jiang, D. Xi, C. Sun, J. Guan, M. He and L. Xiao, *Tetrahedron Lett.*, 2015, **56**, 4868.
- A. Wakamiya, T. Murakami and S. Yamaguchi, *Chem. Sci.*, 2013, **4**, 1002.
- (a) M. Nakamura, H. Tahara, K. Takahashi, T. Nagata, H. Uoyama, D. Kuzuhara, S. Mori, T. Okujima, H. Yamada and H. Uno, *Org. Biomol. Chem.*, 2012, **10**, 6840; (b) M. Nakamura, M. Kitatsuka, K. Takahashi, T. Nagata, S. Mori, D. Kuzuhara, T. Okujima, H. Yamada, T. Nakae and H. Uno, *Org. Biomol. Chem.*, 2014, **12**, 1309.
- H. Yokoi, N. Wachi, S. Hiroto and H. Shinokubo, *Chem. Commun.*, 2014, **50**, 2715.
- (a) S. Rihm, M. Erdem, A. D. Nicola, P. Retailleau, and R. Ziessel, *Org. Lett.*, 2011, **13**, 1916; (b) A. B. Nepomnyashchii, M. Bröring, J. Ahrens, and A. J. Bard, *J. Am. Chem. Soc.*, 2011, **133**, 8633; (c) Y. Hayashi, S. Yamaguchi, M. Saito, Y. Cha, D. Kim and H. Shinokubo, *Org. Lett.*, 2011, **13**, 2992.
- (a) M. Grzybowski, K. Skonieczny, H. Butenschön, D. Gryko, *Angew. Chem., Int. Ed.*, 2013, **52**, 9900; (b) C. Jiao, K. Huang, Z. Guan, Q. Xu and J. Wu, *Org. Lett.*, 2010, **12**, 4046; (c) W. Zeng, S. Lee, M. Son, M. Ishida, J. Furukawa, P. Hu, Z. Sun, D. Kim and J. Wu, *Chem. Sci.*, 2015, **6**, 2427.
- (a) C. Jiao, L. Zhu and J. Wu, *Chem. Eur. J.*, 2011, **17**, 6610; (b) C. Jiao, K. Huang and J. Wu, *Org. Lett.*, 2011, **13**, 632; (c) L. Zeng, C. Jiao, X. Huang, K. Huang, W. Chin and J. Wu, *Org. Lett.*, 2011, **13**, 6026; (d) Y. Hayashi, M. Obata, M. Tamaru, S. Yamaguchi, Y. Matsuo, A. Saeki, S. Seki, Y. Kureishi, M. Saito, S. Yamaguchi and H. Shinokubo, *Org. Lett.*, 2012, **14**, 866; (e) E. Heyer, P. Retailleau and R. Ziessel, *Org. Lett.*, 2014, **16**, 2330; (f) M. Chua, K. Huang, J. Xu, and J. Wu, *Org. Lett.*, 2015, **17**, 4168.
- R. Li, T. A. Mulder, U. Beckmann, P. D. W. Boyd and S. Brooker, *Inorg. Chim. Acta.*, 2004, **357**, 3360.
- (a) K. Rurack, M. Kollmannsberger and J. Daub, *Angew. Chem., Int. Ed.*, 2001, **40**, 385; (b) O. Buyukcakir, O. A. Bozdemir, S. Kolemen, S. Erbas and E. U. Akkaya, *Org. Lett.*, 2009, **11**, 4644; (c) T. Bura, P. Retailleau, G. Ulrich and R. Ziessel, *J. Org. Chem.*, 2011, **76**, 1109.
- (a) A. B. Nepomnyashchii, M. Bröring, J. Ahrens, and A. J. Bard, *J. Am. Chem. Soc.*, 2011, **133**, 19498; (b) M. Bröring, R. Krüger, S. Link, M. Kleeberg, S. Köhler, X. Xie, B. Ventura, L. Flamigni, *Chem. Eur. J.*, 2008, **14**, 2976; (c) B. Ventura, G. Marconi, M. Bröring, R. Krüger and L. Flamigni, *New J. Chem.*, 2009, **33**, 428; (d) S. Knippenberg, M. V. Bohnwagner, P. H. P. Harbach and A. Dreuw, *J. Phys. Chem. A*, 2015, **119**, 1323.
- (a) J. Ahrens, B. Haberlag, A. Scheja, M. Tamm and M. Bröring, *Chem. Eur. J.*, 2014, **20**, 2901; (b) J. Ahrens, B. Böker, K. Brandhorst, M. Funk and M. Bröring, *Chem. Eur. J.*, 2013, **19**, 11382. (c) H. Yokoi, S. Hiroto and H. Shinokubo, *Org. Lett.*, 2014, **16**, 3004; (d) Y. Cakmak and E. U. Akkaya, *Org. Lett.*, 2009, **11**, 85.
- (a) Y. Cakmak, S. Kolemen, S. Duman, Y. Dede, Y. Dolen, B. Kilic, M. Kostereli, L. T. Yildirim, A. L. Dogan, D. Guc and E. U. Akkaya, *Angew. Chem. Int. Ed.*, 2011, **50**, 11937; (b) W. Pang, X.-F. Zhang, J. Zhou, C. Yu, E. Hao and L. Jiao, *Chem. Commun.*, 2012, **48**, 5437; (c) W. Wu, X. Cui and L. Zhao, *Chem. Commun.*, 2013, **49**, 9009.
- (a) N. Saki, T. Dinc and E. U. Akkaya, *Tetrahedron*, 2006, **62**, 2721; (b) M. Bergström, I. Mikhalyov, P. Häggglöf, R. Wortmann, T. Ny and L. B.-J. Johansson, *J. Am. Chem. Soc.*, 2002, **124**, 196.